

## SURFACE PROPERTIES OF ILLITE-SMECTITE MINERALS AS DETECTED BY INTERACTIONS WITH RHODAMINE 6G DYE

V. ŠUCHA<sup>1</sup>, A. CZÍMEROVÁ<sup>2,\*</sup>, AND J. BUJDÁK<sup>2</sup>

<sup>1</sup> Department of Geology of Mineral Deposits, Comenius University, Mlynská dolina G, 842 15 Bratislava, Slovak Republic

<sup>2</sup> Institute of Inorganic Chemistry, Slovak Academy of Science, SK-845 36, Bratislava, Slovak Republic

**Abstract**—Interactions between smectite clay minerals and various organic dyes have been studied extensively, but little information has accumulated from dye interactions with mixed-layer illite-smectite (I-S) minerals, especially regarding relationships with clay layer expandability, layer charge, particle size/shape, and molecular aggregation of organic dye molecules. The purpose of this study was to investigate the surface interactions of a set of mixed-layer illite-smectites from different geological environments with Rhodamine 6G dye. The samples used have different amounts of expandable smectite interlayers, different particle size and/or shape, and different layer-charge density at the surface. Five smectites with differences in layer charge and some non-expandable layer silicates were also tested. The interactions detected by UV-vis spectroscopy show no reaction between R6G and non-expandable minerals (kaolinite, mica), and intense reactions forming H-aggregates and monomers with smectites and illite-smectites. The intensity of H-aggregate formation increases with increase in the layer charge of smectites. Mixed-layer illite-smectites interact with R6G more intensely than do smectites. H-aggregate and monomer formation increases with the illitization process for randomly ordered illite-smectites ( $R = 0$ ) and decreases in the course of illitization for the ordered illite-smectites ( $R > 0$ ).

**Key Words**—Clay Surface Properties, Illite-smectite, Layer Charge, Rhodamine 6G, Smectite, UV-vis Spectroscopy.

### INTRODUCTION

The interaction of layered silicates with various organic dyes has been studied extensively for several decades and was summarized recently in reviews by Bujdák (2006) and Takagi *et al.* (2006). The hybrid materials based on inorganic hosts and supramolecular assemblies of organic dyes, where the components are nm sized, are of much interest in optoelectronics and photonics (del Monte *et al.*, 1999, 2000). Such materials have exhibited considerable utility in non-linear optics (Sanchez *et al.*, 2003), in the development of solid organic lasers (Sanchez *et al.*, 2005), and for optical-data storage media (Schulz-Ekloff, 2002). The interaction of clays and dyes are used for better understanding of clay-surface properties. The adsorbed molecules of some organic dyes can act as molecular sensors or indicators characterizing the parameters of the clay-mineral surface, such as acidity or layer charge (*e.g.* Bujdák and Komadel, 1997; Bujdák 2006).

Dye cations are adsorbed on clay particles through ion exchange and their distribution on the clay surface depends on the negative layer charge. Dye molecular aggregation accompanying the adsorption depends on the distribution of dye cations on the surface, which can be monitored by visible-region absorption spectroscopy.

The formation of dye molecular aggregates on clay surfaces was first mentioned for methylene blue (MB) by Bergman and O'Konski (1963). Since then, many authors have dealt with the interactions of various cationic dyes and clay minerals. The effects of various parameters such as particle size, dye loading, pH of the dye solution, dye concentration, swelling properties, and the nature of the exchangeable cations (Cenens and Schoonheydt, 1988; Neumann *et al.*, 2002; Bergman and O'Konski, 1963; Bujdák *et al.*, 2002; Breen and Loughlin, 1994; Yariv and Lurie, 1971; Czímerová *et al.*, 2004) have been investigated.

The significant effect of layer-charge density on MB molecular aggregation was discovered by Bujdák and Komadel (1997) and Bujdák *et al.* (1998) who characterized the spectra based on the systems of MB in the dispersions of a series of reduced-charge smectites. The specimens in the series had different layer charges, while other parameters (particle size, impurities, type of exchangeable cations, *etc.*) were kept constant. The larger H-aggregates were formed predominantly on the surfaces of high-charge smectites. In general, the H-aggregates are typical of a sandwich-type molecular structure. The reduction of the layer charge led to a decrease in the number of molecular aggregates in favor of dimers and monomers. Later, Bujdák *et al.* (2002) and Czímerová *et al.* (2006) used several types of smectites to verify the influence of the layer charge in comparison with the other parameters. The smectite samples used were different not only in terms of layer charge, but also in terms of their structure and composition. The spectral

\* E-mail address of corresponding author:  
adriana.czimerova@savba.sk  
DOI: 10.1346/CCMN.2009.0570308

properties of these systems were very similar to those described for the series of reduced-charge smectites and can be interpreted in a similar way.

Similar phenomena have been observed for other cationic dyes, *e.g.* cyanines and phenothiazine dyes (Bujdák, 2006). Bujdák *et al.* (2004) described the effect of the layer charge on the aggregation of rhodamine dyes.

In the present study, the interactions between mixed-layer illite-smectite (I-S) minerals and Rhodamine 6G (R6G) dye cations are elucidated. The main objective was to determine experimentally the relationship between the expandability (percentage of expandable smectite interlayers), layer charge, particle size/shape, and molecular aggregation of R6G molecules. On the basis of this approach, some conclusions are drawn about the potential use of R6G as a molecular sensor characterizing the changes in I-S surface properties in nature.

## MATERIALS

Sets of different clays were used to study the relationships between the layer charge and the organization of R6G molecules on the clay surface. The characteristics of all the clays used in this study are summarized in Table 1.

### *Non-expandable clays*

Three samples – one of kaolinite and two of illite with 0% expandability, as measured by the X-ray diffraction (XRD) peak-position method – were used as ‘reference’ samples to assess the interaction of R6G cationic dye with non-expandable minerals. The kaolinite sample (HP) is from the Horná Prievrana residual deposit which originated by *in situ* weathering of Paleozoic rhyolites and phyllites (Kraus, 1989). The illite samples are N504, from anchimetamorphic Permian shales of the Northern Gemicicum, western Carpathians, Slovakia (Šucha *et al.*, 1990), and R61, of anchimetamorphic origin from the Paleozoic shales situated under Miocene sedimentary filling of the East Slovak Basin (Šucha *et al.*, 1993).

### *Smectites*

Five smectite samples from Jelšový Potok, Slovakia (Kraus *et al.*, 1994); Texas, USA (STx – Source Clays Repository of The Clay Minerals Society); Cheto, Arizona, USA (SAZ – Source Clays Repository of The Clay Minerals Society); Kinney, USA; and Otay, USA (Eberl *et al.*, 1986) were selected because of their differences in layer charge (Table 1).

### *Mixed-layer illite-smectites*

Three series of mixed-layer I-S from diagenetic and hydrothermal environments were used. Two series from buried Miocene claystones and bentonites are from the

East Slovak Basin (Šucha *et al.*, 1993; Honý *et al.*, 2004). The samples represent the depth interval between 600 m and 2800 m with XRD expandabilities between 8% and 80%. The third set is from the hydrothermal clay deposit of Dolná Ves, central Slovakia (Šucha *et al.*, 1992, 1996). Illite-smectites here were formed by the hydrothermal alteration of the original smectites. The XRD expandability ranges between 8 and 45%.

Three individual I-S samples were selected because of significant variations in their particle shape: I-S from Le Puy, France, with barrel-shaped particles (Gabis, 1963, Rajec *et al.*, 1999); ‘hairy’ I-S (particles are filament-shaped – elongated parallel to one crystallographic axis) which originated in the pore spaces of Triassic sandstones of Poland (Środon and Elsass, 1994); and RM30 – hydrothermal ‘platy’ (large *a*, *b* dimensions) I-S from the San Juan Mountains, USA (Eberl *et al.*, 1987).

High-purity Rhodamine 6G was purchased from Lambda Physik GmbH.

Table 1. Percentage of the maximum expandability (% $S_{MAX}$ ) of the samples used.

Sample	% $S_{MAX}$ (%)
<i>Smectites</i>	
JP	100
Cheto	100
Kinney	100
Texas	100
Otay	100
<i>Diagenetic illite-smectites</i>	
BP	95
R15	85
R21	83
Loz1/9	78
R36	35
R45	20
Ptr10	71
Cic18	62
Cic12	41
Cic8/11	45
<i>Hydrothermal illite-smectites</i>	
DV4	47
DVS	42
DV1555	37
DV1602	26
DV1603	24
RM30	10
<i>Special illites</i>	
Hairy	13
Le Puy	28
<i>Non-expandable clays</i>	
HP kaolinite	0
N504 illite	0
R61 illite	0

## EXPERIMENTAL

The Na-saturated, <2 µm fraction of each sample was used. These were prepared from aqueous dispersions of the raw clay material, obtained by an ultrasonic disaggregation treatment (20 kHz, 400 W, 5 min). Prior to size separation, the clays were treated with sodium acetate buffer, H<sub>2</sub>O<sub>2</sub>, and sodium dithionite (Jackson, 1975) to remove organic matter and free Fe (oxyhydr)oxides. Excess salts were removed by dialysis. Water and Rhodamine 6G solution ( $10^{-5}$  mol dm<sup>-3</sup>) were added with stirring to obtain R6G-clay dispersions with final R6G and clay concentrations of  $5 \times 10^{-6}$  mol dm<sup>-3</sup> and  $5 \times 10^{-2}$  g dm<sup>-3</sup>, respectively. The visible spectra of R6G-clay dispersions were recorded using a UV-vis spectrophotometer (Varian Cary 100). The spectra were measured 24 h after the R6G solution had been mixed with the clay dispersion. For the model reaction with Jelšový Potok montmorillonite, a series of reaction times between 1 min and 4 days was also tested. The spectra of the clay dispersions without R6G were subtracted from the R6G-clay spectra in order to obtain the spectra specific to the R6G adsorbed. The positions of spectral bands were determined and relative amounts of the species were estimated or compared by second derivatives of the UV-vis spectra. The types of R6G species formed in the clay dispersions, together with the band positions used for their identification, were tabulated (Table 2).

The majority of the spectra for systems based on the dispersions of R6G and clay minerals consist of broad, overlapping bands. The baseline absorption increased non-linearly due to light scattering from the clay-mineral particles, which was affected by the size and shape of the particles as well as by the ratios of swelling/non-swelling phases.

Second-derivative spectroscopy is the most sensitive method for characterizing the electronic structure of the adsorbed R6G species. The second-derivative spectra (SDS) were used to characterize the optical properties of the dye/clay mineral systems due to the greater sensitivity and the better resolution of the broad overlapping absorption bands, which also circumvented problems with the baseline (Antonov and Nedeltcheva, 2000). Maximum absorbance was detected as the minima of negative peaks in SDS, the standard means of determining peak positions for the spectra consisting of

broad bands with non-zero baselines. The SDS also reflect quantitative characteristics of the species. The concentrations of the species are proportional to the areas or amplitudes of the negative peaks (Antonov and Nedeltcheva, 1996), which can be used to estimate or compare the amounts of the same species formed in various reaction systems.

## RESULTS AND INTERPRETATIONS

*Stability of the complex*

The adsorption of dye cations on a clay-mineral surface is a relatively quick process, but the equilibrium of dye molecular aggregation is mostly achieved after longer reaction times (Bujdák *et al.*, 2004). The stability of adsorbed R6G molecular assemblies with time was tested using spectra measured after 1 min, 3, 6, 24, 48, 72, and 96 h, respectively. In the first experiment, Jelšový Potok montmorillonite was used as the clay mineral. The SDS (Figure 1) revealed that an equilibrium or steady-state condition was reached within 24 h, after which time no significant changes in the spectra were detected. Based on this experiment, the spectrum measured 24 h after the contact between the clay minerals and the dye was used as the reference for all samples.

The SDS for R6G-Jelšový Potok montmorillonite dispersions consist of three negative bands. Two change significantly with time, indicating the presence of two main species of R6G in the dispersions being formed or decomposing during the reaction. The isolated cations of the dye, which absorbed near 535 nm, were dominant mainly at the beginning of the reaction (Figure 1). With aging of the dye/clay mineral dispersion, the amount of isolated cations decreased in favor of the H-aggregates, which absorbed at the smallest wavelengths (460 nm). After 24 h, only ~50% of the initially formed, isolated dye cations remained in the system. The decreased intensity of the negative band, assigned to the monomer, was twice as great as the increased intensity in the band associated with the H-aggregates, indicating significantly greater absorptivity of the isolated cations compared to the H-type molecular assemblies. This is consistent with the theory of exciton coupling and other observations (Cenens and Schoonheydt, 1988). Little absorption was observed at 495 nm in the SDS, which is assigned to the H-dimers or to forbidden transitions in the isolated cations, *i.e.* 0–1 vibronic transitions (Bergman and O'Konski, 1963), and any absorption at this wavelength was scarcely detectable in the absorption spectra. The changes in this band were detectable only at the very beginning of the reaction.

Table 2. Band position for species of R6G adsorbed on clay. Assignments are from Bujdák *et al.* (2004).

$\lambda$ (nm)	Species
500–466	H-aggregates
498 (525)	H-dimers
535–540	Monomer

## SPECTRA OF NON-EXPANDABLE CLAY MINERALS

No molecular aggregation of R6G was detected in the dispersions of kaolinite HP and illites N504 and R61

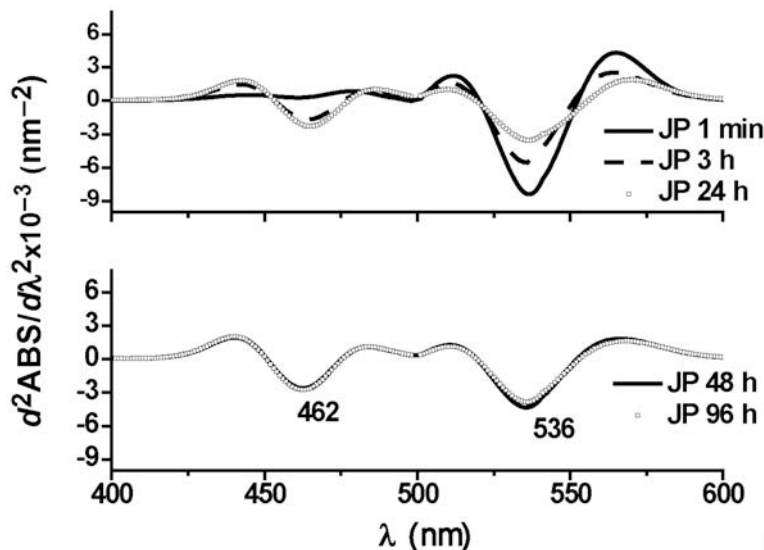


Figure 1. SDS of R6G in the presence of the dispersion of Jelšový Potok montmorillonite measured at various times (1 min – solid line; 3 h – dashed line, 24 h – open squares, 48 h – solid line, 96 h – open squares) after mixing the dye solution with montmorillonite dispersion.

(Figure 2). The resulting SDS, with a characteristic transition at 528 nm, was unchanged with time (not shown) and were only slightly different from a spectrum of R6G solution without any clay admixture. The bands assigned to the monomer were shifted to slightly larger energies (528 nm) due to specific interactions with clay particles. The baseline due to strong light scattering from non-swelling particles could also contribute to the shifts of the bands. Another band at 490 nm is probably related to a vibronic transitional component, as described above for the Jelšový Potok montmorillonite.

The SDS in Figure 2 indicate the absence of R6G H-aggregates in the dispersions of non-expandable clay minerals. This supports the hypothesis that the formation of dye molecular assemblies takes place at basal surfaces. Few basal surfaces are accessible in the non-expandable minerals compared with expandable smectites – attested by the total surface areas measured by the EGME (ethyleneglycol monoethyl ether) technique or calculated from the mean thickness of the particles (Rajec *et al.* 1999). These results are also consistent with another study (Bujdák *et al.*, 2002) dealing with the

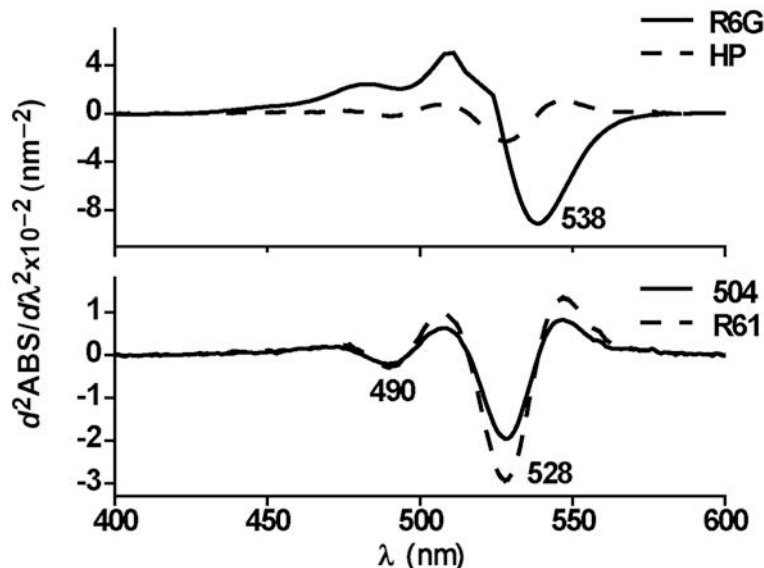


Figure 2. SDS calculated from the absorption spectra of R6G (solid line) and R6G in the presence of non-swelling minerals [HP – kaolinite Horná Prievrana (dashed line), illites 504 (solid line), and R61 (dashed line)] measured 24 h after mixing the components.

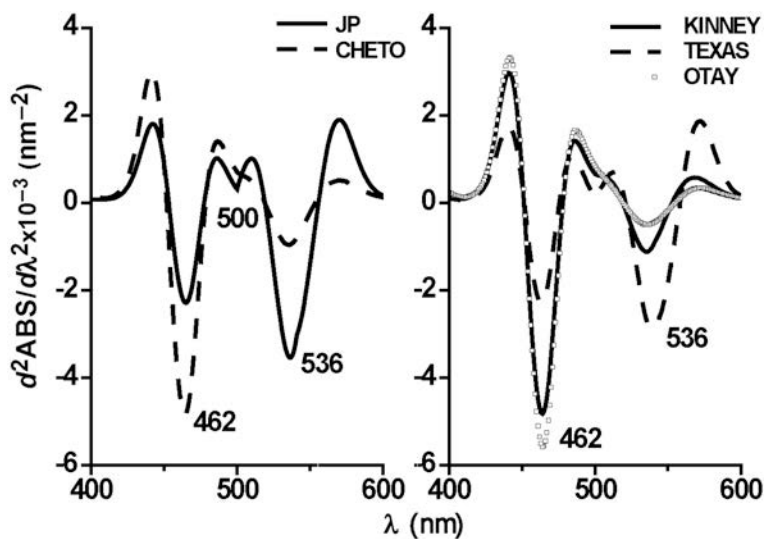


Figure 3. SDS calculated from the absorption spectra of R6G in the presence of various montmorillonites [JP (solid line), Cheto (dashed line), Kinney (solid line), Texas (dashed line) and Otay (open squares)] measured 24 h after mixing the components.

molecular aggregation of MB in the dispersions of montmorillonites with chemically modified edges of clay mineral particles.

#### Smectite spectra

The SDS of R6G mixed with five smectite samples of differing layer charge show significant changes (Figure 3) in comparison with that of dye solution alone (Figure 2). The R6G with the smectites of lesser layer charge (JP and Texas) absorbed strongly at ~535 nm, characteristic of the dye monomer. Less intense peaks at 460 nm are assigned to the H-aggregates. The SDS of R6G with smectites of greater layer charge (Otay, Cheto, Kinney) were characterized by relatively small peaks attributed to the monomer (535 nm) and more intense negative peaks of the H-aggregates (460 nm). The SDS for the colloidal dispersions with Cheto and Kinney smectites were almost identical, whereas the spectrum recorded for the Otay smectite dispersion indicated the smallest amount of isolated dye cations and the largest amount of the H-aggregates. The spectra of the selected smectites of differing layer charge clearly show the relationship between the layer charge and the amplitude of the peak at 462 nm, characteristic of the H-aggregates (Figure 4). The greater the layer charge of the smectite, the larger the number of H-aggregates (460 nm) and the smaller the amount of monomer (535 nm). This fits well with results of previous studies, including the trends observed with other cationic dyes (Bujdák and Komadel, 1997; Bujdák *et al.*, 1998, 2002; Czímerová *et al.*, 2006).

#### Illite-smectite spectra

The R6G-I-S spectra were analyzed. The I-S samples were from different sources and had different

I (non-expandable)/S (expandable) ratios. As for the smectites, the formation of up to three main R6G species occurred in the I-S colloidal dispersions (Figures 5–8). The positions and assignments of the peaks were identical to those discussed above. An absorption peak at greater wavelength (550–560 nm), which occurs in some I-S dispersions, had also been observed in previous studies, *e.g.* for the colloids of montmorillonites with a significantly reduced charge (Bujdák *et al.*, 2004). Similarly, this form was detected when R6G cations were embedded in silica gel and attributed to the J-aggregates with head-to-tail structure (Kikteva *et al.*, 1999).

Although all the I-S specimens used in this study exhibited absorption bands at similar wavelengths, important differences in the amplitudes of the SDS

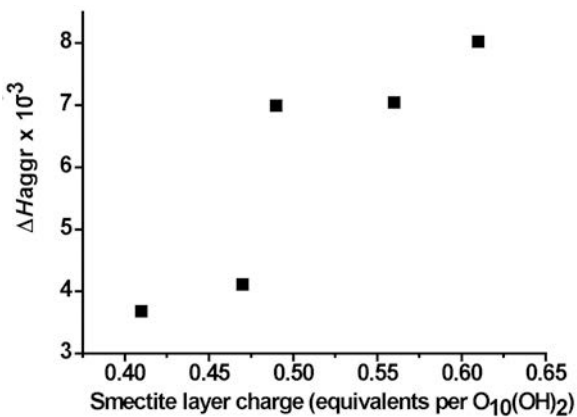


Figure 4. Relationship between the amplitudes calculated from SDS at 462 nm (H-aggregates) and the layer charge of montmorillonites.  $\Delta H_{\text{aggr}}$  represents the amplitude of the SDS at 462 nm.

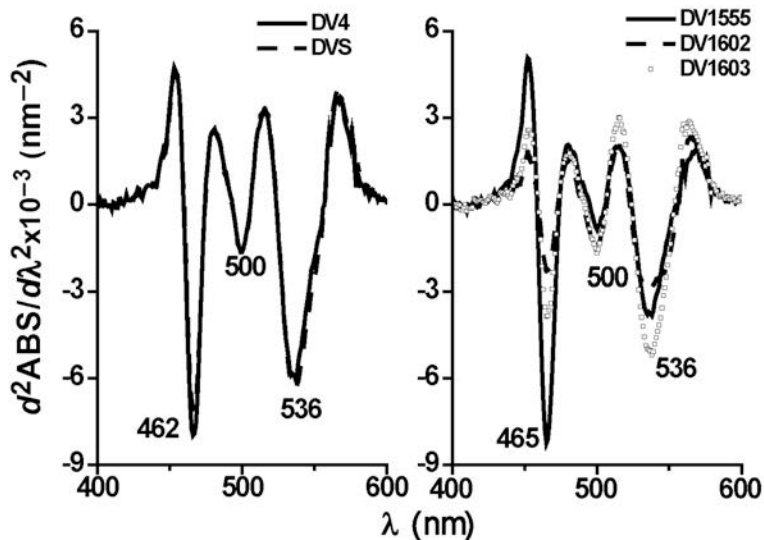


Figure 5. SDS calculated from the absorption spectra of R6G in the presence of hydrothermal illite-smectite samples from Dolná Ves deposit [DV4 (solid line), DVS (dashed line), DV1555 (solid line), DV1602 (dashed line) and DV1603 (open squares)] measured 24 h after mixing the components. The  $\%S_{\text{MAX}}$  increases in the order DV1603  $\approx$  DV1602, DV1555, DVS, DV4.

were observed. The possibility of a systematic relationship between the SDS amplitudes and the properties of mixed-layer I-S, namely the expandability and particle shape, was explored. The expandability effect was observed in the experiments using pure illites and kaolinite, as discussed above. Expandability defined as the number of expandable (smectite) interlayers in I-S is the most frequently used. It can be measured by two approaches. The first uses the XRD peak-position technique where the positions of peaks after saturation with ethylene glycol are measured and compared with the calculated XRD patterns (e.g. Šrodoň, 1984). The

amount of expandable interlayers is expressed as  $\%S_{\text{XRD}}$ . The second approach is based on measurement of the thickness of I-S particles by transmission electron microscopy (TEM) (Šrodoň *et al.*, 1990; Šucha *et al.*, 1996). A systematic difference exists between these two approaches – measurement by TEM is referred to as maximum expandability,  $\%S_{\text{MAX}}$ , and gives systematically larger values. The basal surfaces at the top and the bottom of each mixed-layer crystal are included in this measurement which would not be recognized by the XRD method (for more details see Šrodoň *et al.*, 1990). The maximum expandability expresses the surface

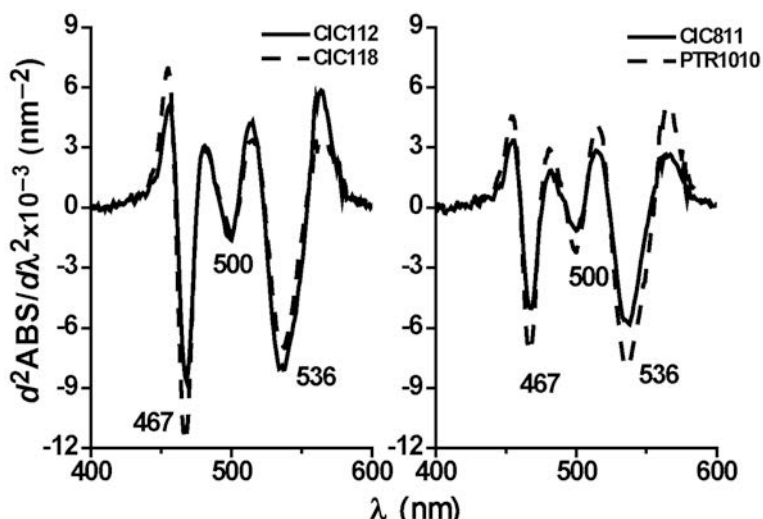


Figure 6. SDS calculated from the absorption spectra of R6G in the presence of illite-smectite from bentonites of diagenetic origin from the East Slovak Basin [CIC112 (solid line), CIC118 (dashed line), CIC811 (solid line), PTR1010 (dashed line)] measured 24 h after mixing the components.

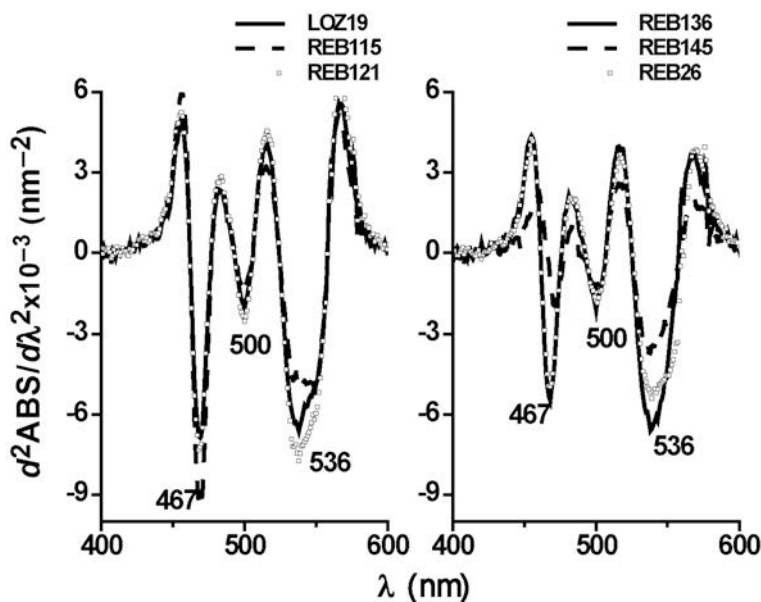


Figure 7. SDS calculated from the absorption spectra of R6G in presence of illite-smectite from shales and claystones of the East Slovak Basin [LOZ19 (solid line), REB115 (dashed line), REB121 (open squares), REB136 (solid line), REB145 (dashed line) and REB26 (open squares)] measured 24 h after mixing the components.

properties of I-S better, as it is directly related to the total surface areas of the clays.

The most homogeneous series of I-S used in the study to test the relationship between the expandability and SDS amplitude of R6G-clay mineral mixtures is from Dolná Ves hydrothermal deposit (Figure 5). These I-S specimens are of the same hydrothermal origin with very limited variations in the chemical composition and particle shape. For all the samples in this series, the measurements of both  $\%S_{XRD}$  and  $\%S_{MAX}$  were available (Šucha *et al.*, 1996). The  $\%S_{MAX}$  varies between 10 and 47%, clearly with good ordering ( $R > 0$ ). All the

samples from Dolná Ves I-S (Figure 9) yielded a direct relationship between the SDS amplitude for the band assigned to the H-aggregates and the  $\%S_{MAX}$ . The amplitude, as well as the area, of this band, decreased with decreases in expandability. Only two samples of the six were slightly off the line of the linear regression, which fits well with the logic of the relationship between the formation of the aggregate and the basal surface area. The area is significantly smaller in samples with less expandability. The amplitudes of the three samples with the greatest expandability were significantly greater than the amplitudes of the smectites with the greatest layer

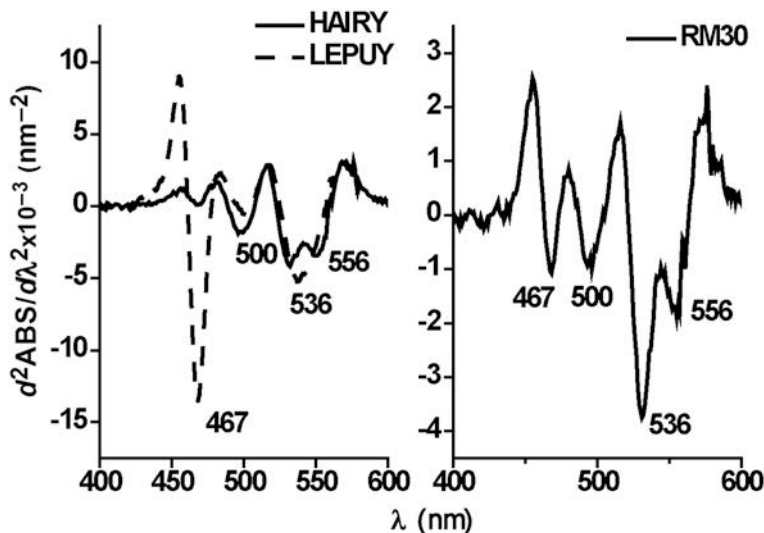


Figure 8. SDS calculated from the absorption spectra of R6G in the presence of illites 'hairy' (solid line), Le Puy (dashed line), and RM30 (solid line) measured 24 h after mixing the components.

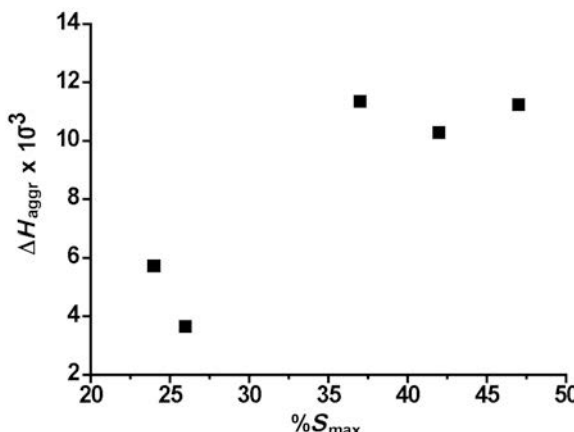


Figure 9. Relationship between the amplitudes in SDS at 462 nm and maximum expandability of the hydrothermal illite-smectites from Dolná Ves deposit.  $\Delta H_{\text{aggr}}$  represents the amplitude of the SDS at 462 nm.

charge (compare Figures 3 and 7), which means that the formation of the H-aggregates was controlled by more than just the size of the basal surface.

To better understand the relationship between the expandability and the formation of H-aggregates, two other series of illite-smectites were also used, buried bentonites and buried shales from the East Slovak Basin (Figures 6, 7). The samples represent a large range of expandability between 10 and 80% and both ordering types  $R = 0$  and  $R > 0$ . The samples are less homogeneous than the specimens in the series from Dolná Ves. The greater heterogeneity arises because of their different geological origins. The expandability values of these two series were plotted *vs.* the SDS amplitudes (Figure 10), together with data for all the

other I-S and five smectite samples used in the study.

Interestingly, the illite-smectites are divided into two series according to ordering. One group represents all I-S with ordered structure ( $R > 0$ ) and their behavior was similar to that of the hydrothermal I-S from Dolná Ves (Figure 10); the amplitude increased with increasing expandability. The second group, consisting of I-S of randomly ordered structure ( $R = 0$ ), showed the opposite trend; the amplitude decreased with increasing expandability. Compared with the smectites, the amplitudes representing the H-aggregates for I-S of randomly ordered structure clearly are much greater in spite of the fact that the expandability is significantly less. A similar pattern was observed when the expandability was plotted *vs.* the amplitude of the SDS peak assigned to the monomer (not shown). In this case, the amplitude of the peak increased along with the illitization process at very early stages ( $R = 0$ ) and decreased as illitization proceeded toward ordered I-S structures.

In illite-smectites, therefore, the interactions with R6G are not controlled by the total surface area alone or by the accessible area of the basal surfaces. The intensity of the interactions expressed as the amount of monomer and H-aggregates formed at the surfaces of I-S particles is significantly greater than on smectite particles. Clearly the intensity of the interactions increases with decreased total surface area at the initial stage of illitization and begins to decrease when expandability is  $<\sim 45\%$  (ordered structure). If the H-aggregate formation is linked to the high-layer-charge sites and the monomer to the low-layer-charge sites, the number of both sites increases significantly in the initial stage of illitization. Therefore, the surface properties of the original smectites undergo significant changes at the beginning of the illitization process, changes which trigger the creation of sites with large and small layer charge.

While the majority of illite particles are of platy shape, some exceptions are observed. Two samples used in this study represent two extreme cases – Le Puy illite with barrel-shaped particles, and L-2A-2 ‘hairy’ illite with the particles elongated in the direction of one crystallographic axis. The spectra of these two samples (Figure 8) show the greatest differences of all the samples used in the study. Le Puy has the largest peak assigned to H-aggregates of all the samples studied. This is not proportional to its expandability and is probably linked to the large number of so called ‘kink-sites’ related to crystal edges (Rajec *et al.* 1999). A very elongate L-2A-2 sample has a very small peak related to H-aggregates, which fits well with the expandability percentage of other I-S used in the study (Figure 10). The amplitude of this peak is very close to that of the RM30 sample, a typical representative of platy particles with large *a*, *b* dimensions. This indicates that the *a*, *b* dimensions do not play an important role in the R6G interaction with illite-smectites.

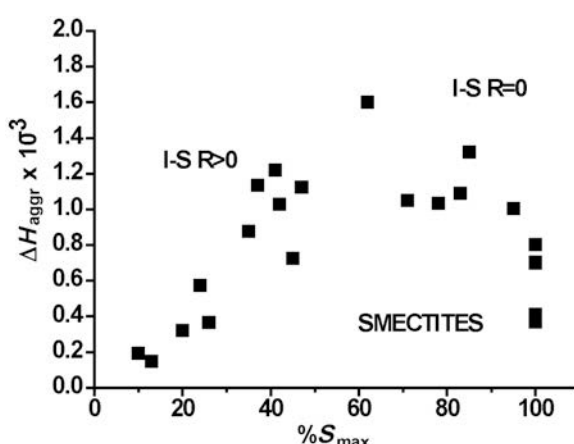


Figure 10. Relationship between amplitudes in SDS at 462 nm and maximum expandability of all smectites and illite-smectites used in the study.  $R = 0$  – randomly ordered illite-smectite layers;  $R > 0$  – illite-smectites with ordered layers.  $\Delta H_{\text{aggr}}$  represents the amplitude of the SDS at 462 nm.

## CONCLUSIONS

Experiments studying the interactions between different types of layer silicates and Rhodamine 6G dye led to the following conclusions:

(1) No molecular aggregates of R6G in the colloids of non-expandable minerals (kaolinite, mica) were formed.

(2) Intense interaction between smectites of different layer charge and R6G led to the formation of H-aggregates. The extent of formation of H-aggregates increases and the amount of monomer decreases with increase in the layer charge of the smectites.

(3) Mixed-layer illite-smectites interact intensely with R6G. Molecular aggregation is greater than in the case of smectites, particularly for randomly ordered smectites. The intensity of formation of both the H-aggregates and monomer increases with the illitization process for this type of I-S, which may indicate the origin of both the high- and low-charge sites. For ordered I-S, the intensities of the bands decrease during the course of illitization.

(4) The *a*, *b* dimensions of the illite particles do not influence the interactions with R6G significantly, though the presence of kink sites typical of the oval illites (Le Puy) increases the formation of H-aggregates, indicating the existence of a large number of high-charge sites.

(5) The results suggest future applications of organic dyes as molecular sensors for the characterization of the surface properties of clays.

## ACKNOWLEDGMENTS

The study reported here was supported by the Slovak Grant Agency VEGA (grant numbers 2/6180/27 and 2/0089/09).

## REFERENCES

- Antonov, L. and Nedeltcheva, D. (1996) Resolution of overlapping bands – An idea for quantitative analysis of undefined mixtures. *Analytical Letters*, **29**, 2055–2069.
- Antonov, L. and Nedeltcheva, D. (2000) Resolution of overlapping UV-Vis absorption bands and quantitative analysis. *Chemical Society Reviews*, **29**, 217–227.
- Bergman, K. and O'Konski, C. T. (1963) A spectroscopic study of methylene blue monomer, dimer, and complexes with montmorillonite. *Journal of Physical Chemistry B*, **67**, 2169–2177.
- Breen, C. and Loughin, H. (1994) The competitive adsorption of methylene blue on to Na-montmorillonite from binary solution with n-alkyltrimethylammonium surfactants. *Clay Minerals*, **29**, 775–783.
- Bujdák, J. (2006) Effect of the layer charge of clay minerals on optical properties of organic dyes. A review. *Applied Clay Science*, **34**, 58–73.
- Bujdák, J. and Komadel, P. (1997) Interaction of methylene blue with reduced charge montmorillonite. *Journal of Physical Chemistry B*, **101**, 9065–9068.
- Bujdák, J., Janek, J.M., Madejová, J., and Komadel, P. (1998) Methylene blue interactions with reduced-charge smectites. *Clays and Clay Minerals*, **46**, 244–254.
- Bujdák, J., Iyi, N., and Fujita T. (2002) The aggregation of methylene blue in montmorillonite dispersions. *Clay Minerals*, **37**, 121–133.
- Bujdák, J., Iyi, N., and Sasai, R. (2004) Spectral properties, formation of dye molecular aggregates and reactions in rhodamine 6G/layered silicates dispersions. *Journal of Physical Chemistry B*, **108**, 4470–4477.
- Cenens, J. and Schoonheydt R. A. (1988) Visible spectroscopy of methylene blue on hectorite, laponite B and barasym in aqueous suspension. *Clays and Clay Minerals*, **36**, 214–224.
- Czimerová, A., Jankovič, L., and Bujdák, J. (2004) Effect of the exchangeable cations on the spectral properties of methylene blue in clay dispersions. *Journal of Colloid and Interface Science*, **274**, 126–132.
- Czimerová, A., Bujdák, J., and Dohrmann, R. (2006) Traditional and novel methods for estimating the layer charge of smectites. *Applied Clay Science*, **34**, 2–13.
- del Monte, F. and Levy, D. (1999) Identification of Oblique and Coplanar Inclined Fluorescent J-Dimers in Rhodamine 110 Doped Sol-Gel-Glasses. *Journal of Physical Chemistry B*, **103**, 8080–8086.
- del Monte, F.J., Mackenzie, D., and Levy, D. (2000) Rhodamine fluorescent dimers adsorbed on the porous surface of silica gels. *Langmuir*, **16**, 7377–7382.
- Eberl, D.D., Šrodoň, J., and Northrop, H.R. (1986) Potassium fixation in smectite by wetting and drying. Pp. 296–326 in: *Geochemical Processes at Mineral Surfaces* (J.A. Davis and K.F. Hayes, editors). ACS Symposium Series, **323**, American Chemical Society, Washington, D.C.
- Eberl, D.D., Šrodoň, J., Lee, M., Nadeau, P.H., and Northrop, H.R. (1987) Sericite from the Silverton caldera, Colorado: Correlation among structure, composition, origin, and particle thickness. *American Mineralogist*, **72**, 914–935.
- Gabis, V. (1963) Etude mineralogique et geo chimique de la serie sedimentaire oligocene du Velay. *Bulletin de la Societe Francaise de Mineralogie et Cristallographie*, **86**, 315–354.
- Honty, M., Uhlík, P., Šucha, V., Čaplovicová, M., Franců, J., and Clauer, N. (2004) Smectite to illite transformation in salt-bearing volcanoclastics (the East Slovak Basin). *Clays and Clay Minerals*, **52**, 533–551.
- Jackson, M.L. (1975) *Soil Chemical Analysis – Advanced Course*, 2nd edition. Madison, Wisconsin, USA.
- Kikteva, T., Star, D., Zhao, Z.H., Baisley, T.L., and Leach, G.W. (1999) Molecular orientation, aggregation, and order in rhodamine films at the fused silica/air interface. *Journal of Physical Chemistry B*, **103**, 1124–1133.
- Kraus, I. (1989) Kaolín a kaolinitové íly Západných Karpat. *Západné Karpaty. Šeria mineralogia petrografia geochemia metalogenéza*, **13**, Geologick ústav Dionza Stúra, Bratislava, 1–287.
- Kraus, I., Šamajová, E., Šucha, V., Lexa, J., and Hroncová, Z. (1994) Diagenetic and hydrothermal of volcanic rocks into clay minerals and zeolites (Kremnické vrchy Mts., The Western Carpathians). *Geologica Carpathica*, **45**, 151–158.
- Neumann, M.G., Gessner, F., Schmitt, C.C., and Sartori, R. (2002) Influence of the layer charge and clay particle size on the interactions between the cationic dye methylene blue and clays in an aqueous suspension. *Journal of Colloid and Interface Science*, **255**, 254–259.
- Rajec, P., Šucha, V., Eberl, D.D., Šrodoň, J., and Elsass, F. (1999) Effect of illite particle shape on cesium sorption. *Clays and Clay Minerals*, **47**, 755–760.
- Sánchez, C., Lebeau, B., Chaput, F., and Boilot, J.-P. (2003) Optical properties of functional hybrid organic-inorganic nanocomposites. *Advanced Materials*, **15**, 1969–1994.
- Sánchez, C., Julián, B., Belleville, P., and Poppal, M. (2005) Application of hybrid organic-inorganic nanocomposites. *Journal of Material Chemistry*, **15**, 3559–3592.
- Schulz-Ekloff, G., Wohrleb, D., van Duffel, B., and Schoonheydt, R.A. (2002) Chromophores in porous silicas and minerals: preparation and optical properties.

- Microporous and Mesoporous Materials*, **51**, 91–138.
- Šrodoň, J. (1984) X-ray diffraction of illitic materials. *Clays and Clay Minerals*, **32**, 337–349.
- Šrodoň, J. and Elsass, F. (1994) Effect of the shape of fundamental particles on XRD characteristics of illitic minerals. *European Journal of Mineralogy*, **6**, 113–122.
- Šrodoň, J., Andreolli, C., Elsass, F., and Robert, M. (1990) Direct high-resolution transmission electron microscopic measurement of expandability of mixed-layer illite/smectite in bentonite rocks. *Clays and Clay Minerals*, **38**, 373–379.
- Šucha, V., Širáňová, V., and Toman, B. (1990) Illite as indicator of post-sedimentary alteration of the Permian sediments from the Northern Gemicicum. *Geologica Carpathica*, **41**, 547–560.
- Šucha, V., Kraus, I., Mosser, Ch., Hroncová, Z., Soboleva, K.A., and Širáňová, V. (1992) Mixed-layer illite/smectite from Dolná Ves hydrothermal deposit, Kremnica Mountains, The West Carpathians. *Geologica Carpathica*, **43**, 13–19.
- Šucha, V., Kraus, I., Gerthofferová, H., Peteš, J., and Sereková, M. (1993) Smectite to illite conversion in bentonites and shales of the East Slovak Basin. *Clay Minerals*, **28**, 243–253.
- Šucha, V., Šrodoň, J., Elsass, F., and McHardy, W.J. (1996) Particle shape versus coherent scattering domain of illite/smectite: Evidence from HRTEM of Dolná Ves clays. *Clays and Clay Minerals*, **44**, 665–671.
- Takagi, S., Eguchi, M., Tryk, D.A., and Inoue, H. (2006) Porphyrin photochemistry in inorganic/organic hybrid materials: Clays, layered semiconductors, nanotubes, and mesoporous materials. *Journal of Photochemistry and Photobiology C: Photochemistry Reviews*, **7**, 104–126.
- Yariv, S. and Lurie D. (1971) Metachromasy in clay minerals. Part I. Sorption of methylene blue by montmorillonite. *Israel Journal of Chemistry*, **9**, 537–552.

(Received 3 November 2008; revised 10 March 2009;  
Ms. 0223; A.E. J. Stucki)